



HAL
open science

A mass-selective ion transfer line coupled with a uniform supersonic flow for studying ion-molecule reactions at low temperatures

Baptiste Joalland, Nour Jamal-Eddine, D. Papanastasiou, A. Lekkas, Sophie Carles, Ludovic Biennier

► To cite this version:

Baptiste Joalland, Nour Jamal-Eddine, D. Papanastasiou, A. Lekkas, Sophie Carles, et al.. A mass-selective ion transfer line coupled with a uniform supersonic flow for studying ion-molecule reactions at low temperatures. *Journal of Chemical Physics*, 2019, 150 (16), pp.164201. 10.1063/1.5086386 . hal-02149464

HAL Id: hal-02149464

<https://univ-rennes.hal.science/hal-02149464>

Submitted on 1 Jul 2019

HAL is a multi-disciplinary open access archive for the deposit and dissemination of scientific research documents, whether they are published or not. The documents may come from teaching and research institutions in France or abroad, or from public or private research centers.

L'archive ouverte pluridisciplinaire **HAL**, est destinée au dépôt et à la diffusion de documents scientifiques de niveau recherche, publiés ou non, émanant des établissements d'enseignement et de recherche français ou étrangers, des laboratoires publics ou privés.

A mass-selective ion transfer line coupled with a uniform supersonic flow for studying ion–molecule reactions at low temperatures

B. Joalland,^{1, a)} N. Jamal-Eddine,¹ D. Papanastasiou,² A. Lekkas,² S. Carles,¹ and L. Biennier^{1, b)}

¹⁾ *Univ Rennes, CNRS, IPR (Institut de Physique de Rennes) – UMR 6251, F-35000 Rennes, France*

²⁾ *Fasmatech Science & Technology SA, TESPA Lefkippos, NCSR Demokritos, 15310 Athens, Greece*

(Dated: 1 April 2019)

A new approach based on the uniform supersonic flow technique – a cold, thermalized de Laval expansion offering the advantage of performing experiments with condensable species – has been developed to study ion–molecule reactions at low temperatures. It employs a mass-selective radio frequency transfer line to capture and select ions from an adaptable ionization source and to inject the selected ions in the core of the supersonic expansion where rate coefficients and product branching can be measured from room temperature down to ~ 15 K. The transfer line incorporates segmented ion guides combining quadrupolar and octapolar field orders to maximize transmission through the differential apertures and the large pressure gradients encountered between the ionization source (\sim mbar), the quadrupole mass filter ($\sim 10^{-5}$ mbar), and the de Laval expansion (\sim mbar). All components were designed to enable the injection of cations and anions of virtually any m/z ratio up to 200 at near ground potential, allowing for a precise control over the momentum and thermalization of the ions in the flow. The kinetics and branching ratios of a selection of reactions have been examined to validate the approach. The technique will be instrumental in providing new insight on the reactivity of polyatomic ions and molecular cluster ions in astrophysical and planetary environments.

I. INTRODUCTION

Ions are detected in trace amounts in astrophysical environments, ranging from interstellar clouds and star-forming regions to protoplanetary disks and circumstellar envelopes.^{1–4} Nearly 30 positive ions have been discovered in space to date, mostly through radio-astronomy. This inventory has recently been enriched by the detection of negative ions. The six anions identified so far all belong to the chemical families of polyynes and cyanopolyynes.^{5–10} In spite of their rarity, ions play a major role in the chemistry of astrophysical environments because they are highly reactive. In fact, most ion–molecule reactions proceed with large rate coefficients at room temperature and below due to the strong attractive forces between the ion and the permanent or induced dipole of the neutral partner. Ion–molecule reactions have thus been invoked as formation pathways for complex organic molecules.¹¹ Molecular ions have also been found to be the key drivers of chemical processes in cold planetary atmospheres such as Titan’s, where the Cassini Huygens probe has revealed the presence of a variety of large and positive ions (up to $1000 m/q$),^{12,13} and significant amounts of even larger negative ions (up to $13\,800 m/q$).¹⁴ These observations have led to the proposition of a new chemical scheme in which molecular growth starts at high altitude through ion–molecule reactions, leading to a rapid mass gain of macromolecules that ultimately generates aerosol seeds.^{15,16}

The formation and destruction pathways of most interstellar and atmospheric ions under the cold conditions prevalent in these environments are still elusive,^{2–4} although considerable efforts have been devoted to develop new experimental methods. In this realm, a key achievement remains the buffer gas cooling experiments with the 22-pole ion trap of D. Gerlich.¹⁷ With an appropriate combination of trapping time and neutral density, the large and nearly field-free volume of this high-order multipole ion trap is suitable for measuring the low-temperature kinetics of slow reactions such as radiative association.^{18–20} On the other hand, the T. Softley group has demonstrated the possibility for reaching the *ultra-cold regime* with collision energies below the mK by introducing velocity-selected neutrals in a linear Paul trap where laser-cooled ions were confined.^{21,22} Latterly, Paul traps have been coupled to time-of-flight mass spectrometry to make simultaneous measurements on multiple exit channels.^{23,24} Nevertheless, ion traps are in general prone to condensation issues at low temperatures, which often limit their applications to light neutral co-reactants.

The uniform supersonic flow (USF) or CRESU technique, originally developed by J.B. Marquette and B.R. Rowe to explore ion–molecule reactions at low temperatures,²⁵ offers the advantage of a *wall-less* experiment where no condensation occurs in the scrutinized medium. The technique relies on de Laval nozzles designed by solving the nonlinear Navier–Stokes equations for viscous fluids. From these nozzles emerge a dense (typically 10^{16} – 10^{18} cm^{−3}) isentropic core in which temperature, density, and translational velocity are uniform for several tenths of centimeters. Under these highly controlled thermodynamic conditions, ions, neutrals, radicals, and clusters are thermalized by inelastic collisions

^{a)} Electronic mail: joallandb@gmail.com; Current address: Department of Chemistry, Wayne State University, Detroit (MI), USA

^{b)} Electronic mail: ludovic.biennier@univ-rennes1.fr

with the carrier gas and travel for several hundreds of microseconds in the course of which their reactivity can be monitored with diverse spectroscopic and mass spectrometry probes.^{26–32} Today this technique has reached a high degree of transferability and versatility owing to the development of different strategies to obtain stable, non-turbulent pulsed flows that reduce considerably the necessary pumping capacities,^{33–35} and to the design of temperature-tunable de Laval nozzles.³⁶

Our interest in the reactivity of molecular ions in astrophysical and planetary media has led us to report recently on the rate coefficients and branching ratios of reactions of $\text{CN}^- / \text{C}_3\text{N}^-$ ions with the polar molecules HCOOH and HC_3N over the [36–300] K temperature range.^{37–39} To our knowledge, it was the first time the kinetics of bimolecular reactions involving a tetraatomic anion was revealed at low temperatures. The experiments were performed with continuous USFs and an electron gun generating a high energy and high current (200 μA) electron beam crossing the flow transversely. Under this configuration, the production of ions is limited by the availability and properties of the precursors, which must exhibit a sufficient vapor pressure at room temperature (> 10 mbar) and be commercially available or synthesizable. Cations are generated through charge transfer with the ionized carrier gas (Ar^+ , He^+ , N_2^+). In most cases, the process induces heavy fragmentation and makes the kinetic analysis complex and the determination of branching ratios difficult, if not impossible. For anions, which are produced by dissociative electron attachment,⁴⁰ the cross-section for the low-energy electrons generated by the ionization of the buffer gas must be non-null and the process must also lead dominantly to the targeted ion. Taken together, these conditions put strong constraints on the variety of ions that can be studied in the laboratory.

An alternative approach consists in injecting mass-selected ions issued from an external ion source into the core of the uniform supersonic flow as in the first CRESU set-up.²⁵ Similarly to the selected ion flow tube (SIFT) method,⁴¹ only the primary ion of interest and the neutral co-reactant are present in the reaction zone. The method was validated with the study of the ion–molecule reactions $\text{He}^+ + \text{N}_2$, $\text{O}_2^+ + \text{CH}_4$, and $\text{N}^+ + \text{H}_2$ at temperatures of 20 and 70 K. The drawback was that the ion source was incorporated within the de Laval nozzle generating the USF, which had to be changed every time the reaction was investigated at a different temperature. Later on, Speck *et al.* developed a pulsed ion source coupled to a CRESU reaction chamber and independent of the nozzle design, although this time the source was not selective in mass.⁴²

To overcome these limitations, we have developed a new approach based on a mass-selective ion transfer line that aims at achieving the same versatility than the SIFT technique while taking advantage of the latest developments in radio frequency (rf) ion guiding. The design of the new experiment is presented in Sec. II and char-

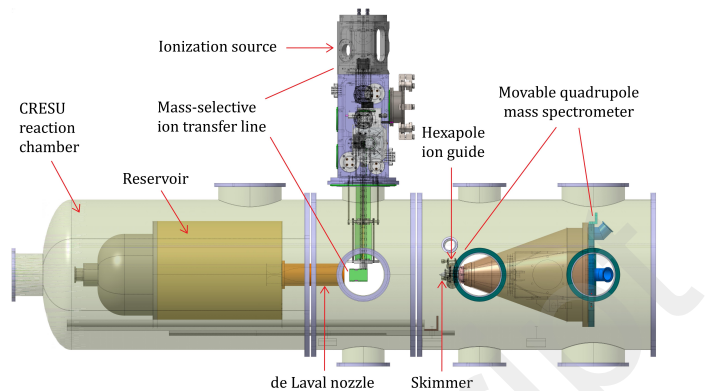


FIG. 1. The CRESU reaction chamber incorporating the new mass-selective ion transfer line. A movable quadrupole mass spectrometer updated with a skimmer / hexapole ion guide combination is used for monitoring ions in the de Laval expansion. High-capacity roots pumps ($> 20\,000\text{ m}^3/\text{h}$) maintain the desired pressure (0.1–2.0 mbar) in the reaction chamber.

acterized in Sec. III. A number of rate coefficients and branching ratios of benchmark reactions were measured and are discussed in Sec. IV. Concluding remarks and future directions are given in Sec. V.

II. DESIGN

An overview of the CRESU reaction chamber with the new mass-selective ion transfer line is shown in Fig. 1. The monitoring of ions along the de Laval expansion is performed by a quadrupole mass spectrometer (QMS) housed in a differentially-pumped conical chamber. The detection chamber, mounted on a position-controlled translating stage, was modified to incorporate a rf hexapole ion guide combined with a molecular beam skimmer to enhance sampling efficiency of reactant and product ions.

A. Mass-selective ion transfer line

The mass-selective ion transfer line is shown in Fig. 2, along with the operating pressure regimes of the different ion optical components. A hollow cathode discharge source operated at ~ 1 mbar is depicted although a variety of ionization sources can easily be implemented. Ions formed near the boundaries of the plasma are transferred through a rf ion funnel and injected into a low pressure region ($< 10^{-2}$ mbar) accommodating a segmented rf ion guide (labeled **1**, 5×2 cm segments). Ions are subsequently introduced into a quadrupole mass filter operated at $\sim 10^{-5}$ mbar with an optimal kinetic energy of 10 eV. In detection mode a mass spectrum is generated using an off-axis electron multiplier. In transmission mode ions are transferred into a second, elongated rf ion guide (labeled **2**, 20×2 cm segments) operated at $\sim 10^{-2}$

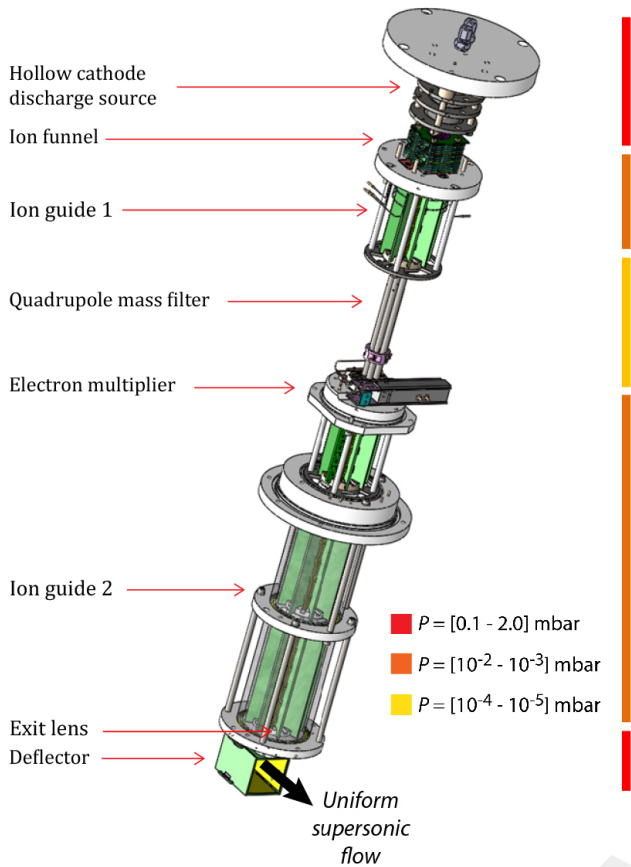


FIG. 2. 3D CAD model of the mass-selective ion transfer line along with pressure regions.

mbar and injected into the reaction chamber through a 2 mm aperture – the exit lens – located near the tip of the de Laval nozzle. The voltage applied to a deflector plate, which is positioned 5 cm from the exit lens, is adjusted to inseminate the isentropic core of the transversal uniform supersonic flow with the mass-selected ions.

Douglas *et al.* studied collisional focusing effects in rf quadrupoles and showed that, provided a low initial ion kinetic energy (1 - 30 eV), the ion transmission through a small aperture at the exit of a quadrupole increases as the pressure increases to reach a maximum near 10^{-2} mbar, i.e. very close to the pressure conditions of ion guides **1** and **2**.⁴³ In addition, collisional focusing was found to be accompanied by significant losses of axial kinetic energy, which is one of the purposes of the new ion transfer line. The ion optics assembly is indeed designed to maintain the exit lens at near ground potential to allow for a precise manipulation of the mass-selected ions in the injection region and their rapid thermalization in the flow (see schematic and potentials in Fig. 3). This required to modify the rf generator driving the quadrupole mass filter (Cyionics) so that it can operate at a floating potential (± 500 V). Both ion guides are designed with an octapolar field at the entrance (three segments) to

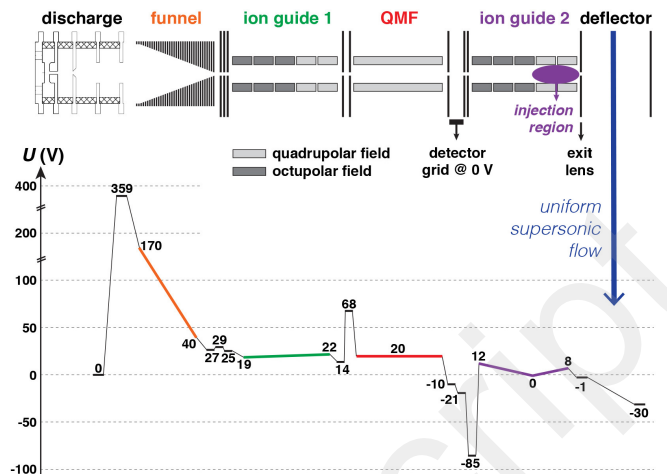


FIG. 3. Schematic of the ion optics assembly and optimized potentials for injecting Ar^+ ions in a uniform supersonic flow. Lens potentials are in black and floating potentials of rf components are in color. Injection region is highlighted in purple.

enhance phase space acceptance and a quadrupolar field at the exit to compress ions radially and thus maintain high transmission through narrow apertures. A weak dc gradient is applied across the segments to counteract collisional cooling and maximize transmission.⁴⁴

All dc and rf potentials applied to the ion transfer line are controlled electronically through our own computer interface. Bipolar dc power supply units (PSU) are employed so that the transfer line can be operated in positive and negative ion mode. A single rf PSU delivering a 2 MHz sinusoidal waveform is used to drive the funnel, the ion guides, and the hexapole integrated upstream the detection QMS (see Sec. II C), while independent dc PSUs are employed to control all static potentials applied to the lens electrodes and to establish the axial dc gradients across the ion guides. In terms of vacuum requirements, the ionization source is backed by a rotary pump (Edwards, 28 m^3/h) and its pressure adjusted with a butterfly valve. Two turbomolecular pumps are used to maintain the ion guides at intermediate pressure (Oerlikon, 360 L/s and Edwards, 70 L/s) and combined with another one (Edwards, 70 L/s) to differentially pump the quadrupole mass filter.

B. Ion trajectory simulations

Ion trajectories were simulated in realistic low-pressure gas flows to better understand the role of scattering on the ion transmission in the injection region (see Figs. 3 and 4). Computations for the diffusive jet formed at the exit lens by the USF carrier gas in the direction of ion guide **2** were performed using the direct simulation Monte Carlo solver⁴⁵ implemented in OpenFOAM. Inlet boundary conditions were obtained by introducing a

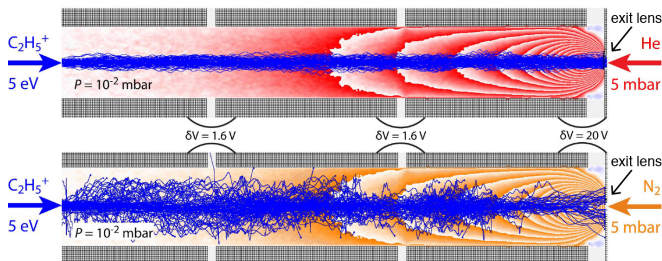


FIG. 4. Simulated trajectories of $C_2H_5^+$ ions in the injection region (last three segments of ion guide **2** / exit lens) superimposed on velocity contours of 50 m/s for He (red) and N_2 (orange) buffer gases with maximum axial and radial speeds of 620 m/s and 360 m/s, respectively.

high pressure inlet boundary at the exit lens and solving the expansion flow along the axis of the ion guide maintained at 10^{-2} mbar. The quadrupole geometry consisted of three 20 mm long equally spaced (1 mm) segments. The inscribed radius of the ion guide was 4 mm and the 10^{-2} mbar pressure boundary was defined at a 7.5 mm radius with reference to the ion optical axis. The post-processed solution for the flow field was introduced in SIMION where ion optical tracing was carried out using a velocity dependent ion–molecule collision model based on ion mobility experimental data.⁴⁶

Two examples of ion trajectory simulations are shown in Fig. 4, where $C_2H_5^+$ ions with kinetic energy of 5 eV are transferred by a weak dc gradient (1.6 V per segment) and accelerated into the higher pressure region by a 20 V difference applied to the 2 mm exit lens. Velocity contours are used to visualize the diffusive jet in the rf ion guide. In the case of an He buffer gas, the ion transmission is $\sim 60\%$, while in the case of N_2 the scattering is much more significant and the transmission falls down to $\sim 5\%$. The simulations indicate that increasing the potential difference between the final segment and the differential aperture improves ion transmission only marginally: an ion transmission of $\sim 80\%$ is achieved for a potential difference of 100 V with the He diffusive jet. Significant losses due to scattering with He were also observed for low-mass ions (≤ 10 amu).

C. Ion sampling and detection

Under the previous configuration with the electron beam as ion source,^{37–39} the ion content in the USF was sampled by an aperture of 80 μm at the tip of the cone detection chamber, while the diameter of a typical isentropic core ranges from 5 mm to 1 cm. A large distance (66 mm) between the tip of the cone and the entrance lens of the QMS led to significant losses of ions. The sensitivity of the detection scheme had therefore to be improved because the ion current generated by the new transfer line lies in the [0.1–1] nA range, i.e. three orders of magnitude lower than with the electron beam. To this

end the combination of a molecular beam skimmer with an hexapole ion guide filling the gap between the cone tip and the QMS was designed. Under CRESU operating conditions, the pressure in the ion guide is maintained in the $[10^{-2}–10^{-3}]$ mbar range through a connection to the roots pumping system of the reaction chamber. The voltage applied to the hexapole is decomposed into a dc component of a few V and a rf component of a few hundreds of V. A 10x larger skimmer (Beam Dynamics 0.8 mm i.d.), gold plated to protect from corrosion, was installed to increase ion transmission by 100x. The new ion sampler was tested with a HCDS directly mounted in front of the detection scheme. The skimmer was polarized by a fraction of V. The application of a potential of 200 V rf amplitude to the hexapole resulted in a further 15x enhancement. The skimmer / hexapole ion guide combination therefore enables us to circumvent in its entirety the lower ion currents generated by the mass-selective ion transfer line.

III. CHARACTERIZATION

We report here on proof-of-concept measurements for the injection of Ar^+ ions. An Ar/He mixture is admitted into the ionization source and the glow discharge (360 V – 1 mA) projects ions through the ion funnel, from which they are captured by the first ion guide before reaching the quadrupole mass filter. The presence of Ar^+ , ArH^+ as well as traces of H_2O^+ , H_3O^+ , and N_2^+ ions was detected, as shown in the inset of Fig. 5. Ar^+ ions were selected and all the dc potentials of the transfer line were adjusted to maximize the ion currents measured on the exit lens, the deflector, and the skimmer of the detection chamber with a picoammeter. The optimized potentials for injection at near ground potential are shown in Fig. 3.

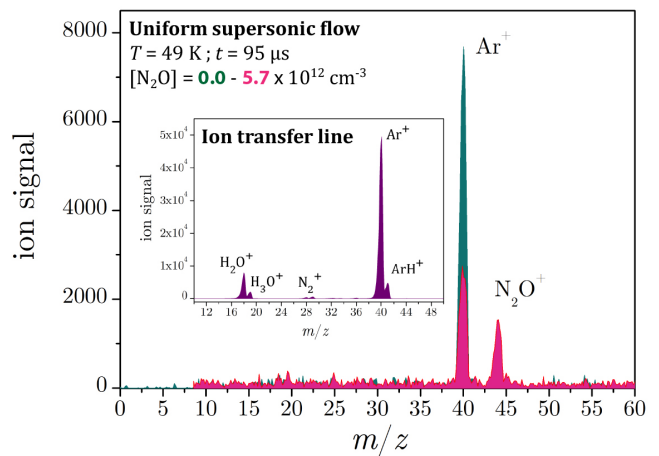


FIG. 5. Mass spectra in a uniform supersonic flow at 49 K insemated by mass-selected Ar^+ ions after a reaction time of 95 μs in absence (green) / presence (pink) of N_2O . Inset: mass spectrum in the ion transfer line for an Ar/He plasma.

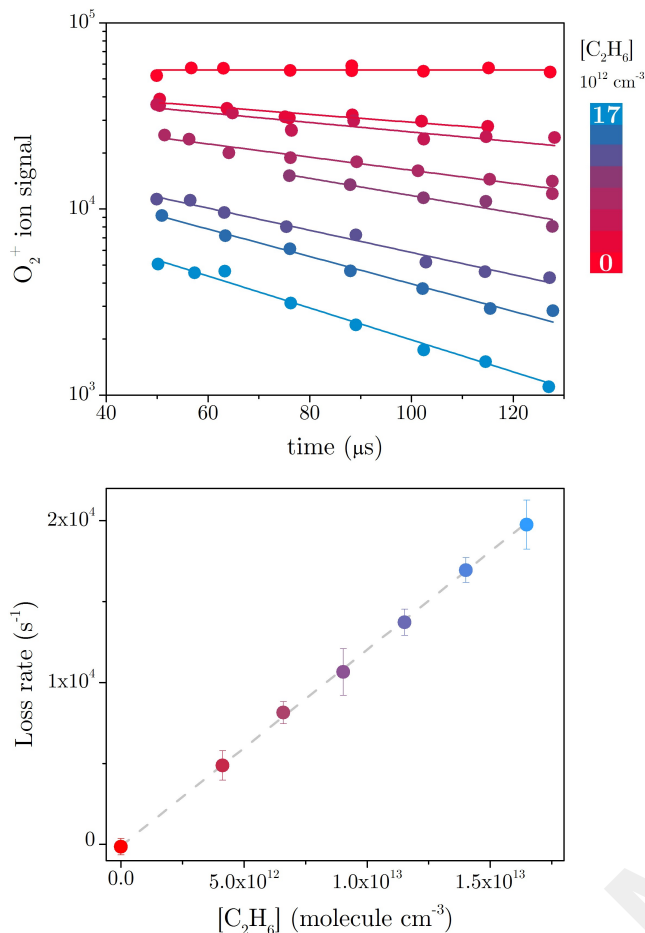


FIG. 6. O_2^+ ion signal at 49 K as a function of time for a range of ethane concentration $[\text{C}_2\text{H}_6]$ (top) and corresponding loss rates as a function of $[\text{C}_2\text{H}_6]$ (bottom), the slope of which determines the rate coefficient of the $\text{O}_2^+ + \text{C}_2\text{H}_6$ reaction.

In practice, the reaction chamber is first filled with the USF buffer gas in a static manner so that one can optimize the settings of the transfer line without consuming all the gas and power necessary for a CRESU experiment.

A current of several hundreds of pA was measured on the exit lens and the deflector for chamber pressure (P_{ch}) of 0.2 to 2.0 mbar, with a maximum at $P_{ch} \sim 1$ mbar. With a de Laval expansion of helium at 49 K demanding that $P_{ch} = 0.77$ mbar, the ion current was monitored on the skimmer at various distances from the exit aperture of the transfer line (from 7 cm to 20 cm, i.e. the effective length of this uniform flow). Applying a voltage of -30 ± 1 V on the deflector allowed for more than 95% of the selected ions to be drifted towards the skimmer. The measurements showed no variations greater than 3–4% along the flow. We found that the current is very sensitive to the voltage applied on the deflector as a change of ± 5 V leads to its complete disappearance. This way, a simple yet fine tuning of the kinetic energy necessary for in-seminating the USF with the selected ions is achieved.

The ion content of the USF was monitored by the mov-

TABLE I. Rate coefficients k compared with previous measurements and Langevin rates.

	T (K)	k ($10^n \text{ molecule}^{-1} \text{ cm}^3 \text{ s}^{-1}$)			$[n]$
		This work	Prev. meas.	Langevin	
$\text{Ar}^+ + \text{C}_2\text{H}_6$	36 ^a	1.20 ± 0.12	0.86^b	1.16	[-9]
	49 ^a	1.33 ± 0.13	-		
	300	-	0.92^c		
	380	-	1.14^d		
$\text{O}_2^+ + \text{C}_2\text{H}_6$	49 ^a	1.21 ± 0.13	-	1.22	[-9]
	300	-	$1.21^e / 1.1^f$		
$\text{Ar}^+ + \text{N}_2\text{O}$	36 ^a	4.6 ± 0.5	-	8.9	[-10]
	49 ^a	5.7 ± 0.9	-		
	72 ^a	4.8 ± 0.6	-		
	300	-	$3.3^g / 3.0^h$		
$\text{Ar}^+ + \text{N}_2$	36 ^a	3.07 ± 0.27	3.00^b	75.5	[-11]
	49 ^a	2.00 ± 0.19	-		
	72 ^a	1.09 ± 0.12	1.30^b		

^a Flow temperatures (± 1 K) determined by impact pressure and laser-induced fluorescence measurements.

^b CRESU with pulsed ion injection by Speck *et al.*⁴²

^c Flowing afterglow experiments by Tsuji *et al.*⁴⁷

^d Selected ion flow drift tube experiments by Praxmarer *et al.*⁴⁸

^e Time-resolved atmospheric pressure ionization mass spectrometry experiments performed in the [238–458] K range by Matsuoka and Ikezoe⁴⁹

^f Selected ion flow tube experiments by Wilson *et al.*⁵⁰

^g Selected ion flow tube experiments by Shul *et al.*⁵¹

^h Ion cyclotron resonance mass spectrometry experiments by Kemper and Bowers⁵²

able QMS incorporating the new ion sampler, as illustrated in Fig. 5 for the $\text{Ar}^+ + \text{N}_2\text{O}$ reaction. Ar^+ is the only ion detected in absence of N_2O while the reaction leads to the appearance of the single product N_2O^+ .

IV. KINETICS AND BRANCHING RATIOS

The rate coefficients k and branching ratios of a set of benchmark ion–molecule reactions were measured at various temperatures with the new mass-selective transfer line and ion sampling scheme. Kinetic data were obtained under pseudo-first order conditions by measuring the loss rates of the mass-selected ions for various concentrations of neutral co-reactant set in excess, as illustrated in Fig. 6 for the $\text{O}_2^+ + \text{C}_2\text{H}_6$ reaction. Rate coefficients are compared with previous measurements and Langevin rates in Table I. Error bars account for statistical and systematic (10%) contributions, the latter finding its origin in uncertainties in the mass flow rates and the reservoir / chamber pressures. The branching ratios reported in Table II were determined at short reaction times to minimize secondary reactions.

Two exoergic ion–molecule reactions involving Ar^+ and O_2^+ with non-polar ethane C_2H_6 were studied. For these reactions, k remains constant as a function of temperature. Previous measurements at 300 K and above have shown a close agreement with Langevin rates,^{49,53}

TABLE II. Branching ratios for the $\text{Ar}^+ + \text{C}_2\text{H}_6$ and $\text{O}_2^+ + \text{C}_2\text{H}_6$ reactions and comparison with previous measurements.

Products	T (K) =	Branching ratios		
		This work ^a	Prev. meas.	
$\text{Ar}^+ + \text{C}_2\text{H}_6 \rightarrow$	T (K) =	49	300 ^b	380 ^c
$\text{C}_2\text{H}_6^+ + \text{Ar}$		0.03	-	-
$\text{C}_2\text{H}_5^+ + \text{H} + \text{Ar}$		0.10	0.08	0.18
$\text{C}_2\text{H}_4^+ + \text{H}_2 + \text{Ar}$		0.23	0.22	0.18
$\text{C}_2\text{H}_3^+ + \text{H}_2 + \text{H} + \text{Ar}$		0.36	0.42	0.38
$\text{C}_2\text{H}_2^+ + 2\text{H}_2 + \text{Ar}$		0.23	0.23	0.20
$\text{CH}_3^+ + \text{CH}_3 + \text{Ar}$		0.05	0.05	0.06
$\text{O}_2^+ + \text{C}_2\text{H}_6 \rightarrow$	T (K) =	49	300 ^d	
$\text{C}_2\text{H}_6^+ + \text{O}_2$		0.26	0.30	
$\text{C}_2\text{H}_5^+ + \text{O}_2 + \text{H}$		0.57	0.55	
$\text{C}_2\text{H}_4^+ + \text{O}_2 + \text{H}_2$		0.17	0.15	

^a Error bars can be estimated by adding systematic (± 0.02) and statistical ($\pm 5\%$) contributions.

^b Flowing afterglow experiments by Tsuji *et al.*⁴⁷

^c Selected ion flow drift tube experiments by Praxmarer *et al.*⁴⁸

^d Selected ion flow tube experiments by Wilson *et al.*⁵⁰

as our new low-temperature results for both reactions. In the case of the $\text{Ar}^+ + \text{C}_2\text{H}_6$ reaction, the branching into the six identified exit channels, for which dissociative charge transfer reactions dominate (97%), agree well with previous flowing afterglow⁴⁷ and selected ion flow drift tube⁴⁸ measurements. In the case of the $\text{O}_2^+ + \text{C}_2\text{H}_6$ reaction, three exit channels leading to C_2H_6^+ (charge transfer) and $\text{C}_2\text{H}_5^+ / \text{C}_2\text{H}_4^+$ (dissociative charge transfer) have been reported previously and their branching ratios measured at 300 K with the SIFT technique.⁵⁰ The results obtained here at 49 K show a remarkable agreement with the SIFT values, suggesting that the branching of this reaction does not, as for the $\text{Ar}^+ + \text{C}_2\text{H}_6$ reaction, depend on temperature over the explored range.

The kinetics of two charge transfer reactions with temperature-dependent rate coefficients was also measured. For the $\text{Ar}^+ + \text{N}_2\text{O}$ reaction, the rate coefficients measured at low temperatures are only slightly higher than the one measured at 300 K because little temperature dependence is expected due to the small dipole moment of N_2O ($\mu = 0.16$ D). The new rates reach about 60% of the Langevin rate, compared to 35% at 300 K. In contrast, k is much smaller than the Langevin rate for the $\text{Ar}^+ + \text{N}_2$ (1-4%) and exhibits a pronounced negative temperature dependence below 140 K although N_2 is non-polar (see Fig. 7). This is due to the competition between two exit channels: $\text{N}_2^+(v=0) + \text{Ar}$, exoergic by 0.18 eV and dominant at $T < 140$ K, and $\text{N}_2^+(v=1) + \text{Ar}$, endoergic by 0.09 eV and dominant at higher temperatures.⁵⁴ The kinetic results are totally consistent with previous SIFT⁵⁵ and CRESU^{42,56} measurements.

Whereas the thermalization of the translational and rotational degrees of freedom is extremely efficient within a uniform supersonic flow owing to its high density – the mean time between collisions with the buffer gas is typically a few tenths of nanoseconds –, the relaxation

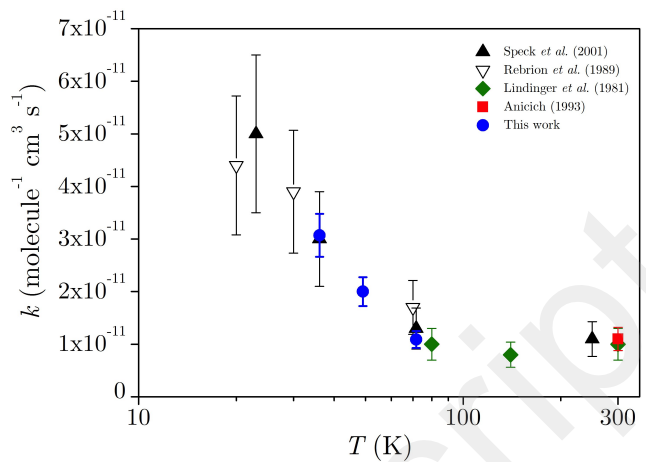


FIG. 7. Rate coefficients for the $\text{Ar}^+ + \text{N}_2$ reaction as a function of temperature. Blue circles: this work. Black triangles: previous CRESU measurements.^{42,56} Green diamonds: SIFT measurements.⁵⁵ Red square: Average room temperature value taken from the review of V.G. Anicich.⁵⁷

of electronic and vibrational excited states of the mass-selected ions must be taken with caution, alike in SIFT studies. Spin-orbit excited states of Ar^+ and vibrational excited states of O_2^+ are indeed likely to be formed in the plasma source. According to Hamdan *et al.*,⁵⁸ the de-excitation rate of $\text{Ar}^+ (^2P_{1/2})$ to $\text{Ar}^+ (^2P_{3/2})$ is equal to $\sim 4 \times 10^{-11}$ molecule⁻¹ cm³ s⁻¹ in He, meaning that the relaxation to the ground state is achieved in the sub-microsecond time scale, i.e. directly in the dense plasma source. For molecular ions, vibrational relaxation may turn out to be slow, in particular in the case of non-polar diatomic molecules with relatively high frequency vibrations.⁵⁹ To settle this debate, the vibrational deactivation of O_2^+ ($v=1, 2$) with different neutral partners was investigated in the laboratory by Böhringer *et al.*⁶⁰ Their experiments showed that only ~ 2 collisions with neutral O_2 are necessary to quench the $v=1$ and $v=2$ states of O_2^+ , making this process very efficient. Ion trajectory simulations with a hard sphere collision model show that O_2^+ ions undergo ~ 800 collisions from their production zone to the funnel exit while only a handful of additional collisions take place in the ion guide. By considering a typical mixing ratio of O_2 in He of 1%, we estimate that O_2^+ ions undergo ~ 8 collisions with neutral O_2 during their travel in the ionization source. This is a conservative number because more sophisticated collision models based on ion mobility data show that the hard sphere model employed here underestimates the collision cross sections for low relative velocities. These simulations therefore suggest that O_2^+ ions are thermalized at the very beginning of the mass-selective ion transfer line. From an experimental viewpoint, the kinetic traces would likely show some curvature in case significant amounts of either spin-orbit excited Ar^+ or vibrationally excited O_2^+ ions were injected.⁶¹ For instance, the effect of vibrational excitation of O_2^+ on the rate coefficient of the charge ex-

change reaction $\text{O}_2^+ + \text{O}_2$ has been shown to enhance the reactivity.⁶² Here the rate coefficients and branching ratios show overall a good agreement with previous work, providing additional evidence for the effective thermalization of the selected ions in the de Laval expansion. We can therefore consider that no excited states of either Ar^+ or O_2^+ were interfering with the kinetic measurements.

The ultimate goal of the apparatus presented here remains the investigation of reactions with large polyatomic ions. Ferguson and coworkers pointed out that vibrational deactivation efficiency is greater for low frequency vibrations, in which a lesser amount of vibrational energy need to be converted into translational energy.⁵⁹ As their neutral precursors will be injected in significant amounts ($\sim 1\%$) in the source, one can very reasonably assume that polyatomic ions will efficiently relax in the plasma chamber itself, leaving little doubt on their good thermalization. Hence, the ion transfer line offers the convenience of preparing mass-selected, ground state ions remotely, restraining the introduction in the uniform supersonic flow of the species of interest only and permitting a simple, robust analysis of low-temperature multichannel kinetic data. Depending on the studied ions, these results do not however preclude for additional spectroscopic measurements to assess the internal energy of ions but common sensitive methods (e.g. laser-induced fluorescence or cavity ring-down spectroscopy) are vain considering the very low density of ions in the flow, leaving only indirect methods such as action spectroscopy.

V. CONCLUSION AND PERSPECTIVES

The new experimental approach presented here – a mass-selective ion transfer line coupled with the uniform supersonic flow technique to measure rate coefficients and branching ratios of ion–molecule reactions at low temperatures – allows for monitoring this class of reactions in a thermalized medium where no condensation takes place and where only the target species are present. The data analysis is made straightforward and the same versatility than the selected ion flow tube technique has been demonstrated while offering new possibilities for investigating ion–molecule reactions in the cold regime. The design of the ion transfer line, which takes advantage of the relatively high pressure in the reaction chamber and of the combination of quadrupolar and octapolar radio frequency field orders, makes possible to concurrently (i) maximize ion transmission through large pressure gradients, (ii) ensure the prompt thermalization of the mass-selected ions, (iii) redirect the ion cloud along the propagation axis of the cold de Laval expansion readily. Provided an efficient ionization source, this new strategy will be dedicated to unveil the low-temperature reactivity of polyatomic ions of astrophysical interest, e.g. $\text{H}-(\text{C}\equiv\text{C})_n^-$ polyynes, and molecular clusters such as micro-solvated ions.

The current apparatus is restricted to He / H_2 uniform supersonic flows because of significant scattering occurring in the injection region. To overcome this limitation, the design of low-density, low-pressure nozzles is underway. A better control over the pressure in the second, elongated ion guide with additional pumping capacity would be also advantageous. Alternatively, the development of a differential aperture with an adjustable diameter – an iris diaphragm for ion optics – to be mounted at the interface between the ion transfer line and the reaction chamber would facilitate the control of the balance between ion transmission, collisional focusing, and scattering over the diversity of conditions imposed by the fluid dynamics of de Laval expansions. Although the present version of the mass-selective ion transfer line has not been designed initially to be coupled with pulsed CRESU flows, we anticipate that this would not require any major adjustment. In both ways – continuous and pulsed – the sensitivity of the detection could be further enhanced by maintaining a higher vacuum in the hexapole ion guide linking the molecular beam skimmer to the entry lens of the quadrupole mass spectrometer.

ACKNOWLEDGMENT

We thank J. Courbe for the mechanical adaptation and J. Thiévin for the data acquisition. We are also grateful to the referees for their valuable comments. This work was supported by the *Agence Nationale de la Recherche* through the AnionCosChem project (ANR-14-CE33-0013) and the national research programs *Physique et Chimie du Milieu Interstellaire* (PCMI) and *Programme National de Planétologie* (PNP) of CNRS/INSU with INC/INP and co-funded by CEA and CNES.

- ¹S. Petrie and D. K. Bohme, “Ions in space,” *Mass Spectrometry Reviews* **26**, 258–280 (2007).
- ²T. P. Snow and V. M. Bierbaum, “Ion chemistry in the interstellar medium,” *Annual Review of Analytical Chemistry* **1**, 229–259 (2008).
- ³M. Larsson, W. D. Geppert, and G. Nyman, “Ion chemistry in space,” *Reports on Progress in Physics* **75**, 066901 (2012).
- ⁴T. J. Millar, C. Walsh, and T. A. Field, “Negative ions in space,” *Chemical Reviews* **117**, 1765–1795 (2017).
- ⁵M. McCarthy, C. Gottlieb, H. Gupta, and P. Thaddeus, “Laboratory and astronomical identification of the negative molecular ion C_6H^- ,” *Astrophys. J. Lett.* **652**, L141 (2006).
- ⁶J. Cernicharo, M. Guélin, M. Agúndez, K. Kawaguchi, M. McCarthy, and P. Thaddeus, “Astronomical detection of C_4H^- , the second interstellar anion,” *Astronomy & Astrophysics* **467**, L37–L40 (2007).
- ⁷S. Brünken, H. Gupta, C. Gottlieb, M. McCarthy, and P. Thaddeus, “Detection of the carbon chain negative ion C_8H^- in TMC-1,” *Astrophysical Journal Letters* **664**, L43 (2007).
- ⁸P. Thaddeus, C. Gottlieb, H. Gupta, S. Brünken, M. McCarthy, M. Agúndez, M. Guélin, and J. Cernicharo, “Laboratory and astronomical detection of the negative molecular ion C_3N^- ,” *Astrophys. J.* **677**, 1132 (2008).
- ⁹J. Cernicharo, M. Guélin, M. Agúndez, M. McCarthy, and P. Thaddeus, “Detection of C_5N^- and vibrationally excited C_6H in IRC+10216,” *Astrophysical Journal Letters* **688**, L83 (2008).

- ¹⁰M. Agúndez, J. Cernicharo, M. Guélin, C. Kahane, E. Roueff, J. Klos, F. Aoi, F. Lique, N. Marcelino, J. Goicoechea, *et al.*, “Astronomical identification of CN^- , the smallest observed molecular anion,” *Astron. & Astrophys.* **517**, L2 (2010).
- ¹¹E. Herbst and E. F. van Dishoeck, “Complex organic interstellar molecules,” *Annual Review of Astronomy and Astrophysics* **47**, 427–480 (2009).
- ¹²J. H. Waite, D. T. Young, T. E. Cravens, A. J. Coates, F. J. Crary, B. Magee, and J. Westlake, “The process of tholin formation in Titan’s upper atmosphere,” *Science* **316**, 870 (2007).
- ¹³F. J. Crary, B. A. Magee, K. Mandt, J. H. Waite Jr, J. Westlake, and D. T. Young, “Heavy ions, temperatures and winds in Titan’s ionosphere: Combined Cassini CAPS and INMS observations,” *Planetary and Space Science* **57**, 1847–1856 (2009).
- ¹⁴A. J. Coates, F. J. Crary, G. R. Lewis, D. T. Young, J. H. Waite, and E. C. Sittler, “Discovery of heavy negative ions in Titan’s ionosphere,” *Geophysical Research Letters* **34**, L22103 (2007).
- ¹⁵J. Žabka, C. Romanzin, C. Alcaraz, and M. Polášek, “Anion chemistry on titan: A possible route to large N-bearing hydrocarbons,” *Icarus* **219**, 161–167 (2012).
- ¹⁶P. Lavvas, R. V. Yelle, T. Koskinen, A. Bazin, V. Vuitton, E. Vigren, M. Galand, A. Wellbrock, A. J. Coates, J.-E. Wahlund, F. J. Crary, and D. Snowden, “Aerosol growth in Titan’s ionosphere,” *Proceedings of the National Academy of Sciences* (2013).
- ¹⁷D. Gerlich, “Ion–neutral collisions in a 22–pole trap at very low energies,” *Physica Scripta* **1995**, 256 (1995).
- ¹⁸S. Barlow, G. Dunn, and M. Schauer, “Radiative association of CH_3^+ and H_2 at 13 K,” *Physical Review Letters* **52**, 902 (1984).
- ¹⁹D. Gerlich and G. Kaefer, “Ion trap studies of association processes in collisions of CH_3^+ and CD_3^+ with $n\text{-H}_2$, $p\text{-H}_2$, D_2 , and He at 80 K,” *The Astrophysical Journal* **347**, 849–854 (1989).
- ²⁰R. Otto, J. Mikosch, S. Trippel, M. Weidemüller, and R. Wester, “Nonstandard behavior of a negative ion reaction at very low temperatures,” *Physical Review Letters* **101**, 063201 (2008).
- ²¹S. Willitsch, M. T. Bell, A. D. Gingell, S. R. Procter, and T. P. Softley, “Cold reactive collisions between laser-cooled ions and velocity-selected neutral molecules,” *Physical Review Letters* **100**, 043203 (2008).
- ²²B. R. Heazlewood and T. P. Softley, “Low-temperature kinetics and dynamics with Coulomb crystals,” *Annual Review of Physical Chemistry* **66**, 475–495 (2015).
- ²³J. Greenberg, P. C. Schmid, M. Miller, J. F. Stanton, and H. Lewandowski, “Quantum-state-controlled reactions between molecular radicals and ions,” *Physical Review A* **98**, 032702 (2018).
- ²⁴T. Yang, A. Li, G. K. Chen, C. Xie, A. G. Suits, W. C. Campbell, H. Guo, and E. R. Hudson, “Optical control of reactions between water and laser-cooled Be^+ ions,” *The Journal of Physical Chemistry Letters* (2018).
- ²⁵B. R. Rowe and J. B. Marquette, “CRESU studies of ion–molecule reactions,” *International Journal of Mass Spectrometry and Ion Processes* **80**, 239–254 (1987).
- ²⁶I. Sims, J.-L. Queffelec, A. Defrance, C. Rebrion-Rowe, D. Travers, P. Bocherel, B. Rowe, and I. W. Smith, “Ultralow temperature kinetics of neutral–neutral reactions. the technique and results for the reactions $\text{CN} + \text{O}_2$ down to 13 k and $\text{CN} + \text{NH}_3$ down to 25 k,” *The Journal of chemical physics* **100**, 4229–4241 (1994).
- ²⁷S. Lee, R. J. Hoobler, and S. R. Leone, “A pulsed laval nozzle apparatus with laser ionization mass spectroscopy for direct measurements of rate coefficients at low temperatures with condensable gases,” *Review of Scientific Instruments* **71**, 1816–1823 (2000).
- ²⁸A. Bonnamy, R. Georges, E. Hugo, and R. Signorell, “Ir signature of $(\text{CO}_2)_n$ clusters: size, shape and structural effects,” *Physical Chemistry Chemical Physics* **7**, 963–969 (2005).
- ²⁹H. Sabbah, L. Biennier, S. J. Klippenstein, I. R. Sims, and B. R. Rowe, “Exploring the role of PAHs in the formation of soot: Pyrene dimerization,” *The Journal of Physical Chemistry Letters* **1**, 2962–2967 (2010).
- ³⁰S. Soorkia, C.-L. Liu, J. D. Savee, S. J. Ferrell, S. R. Leone, and K. R. Wilson, “Airfoil sampling of a pulsed laval beam with tunable vacuum ultraviolet synchrotron ionization quadrupole mass spectrometry: Application to low-temperature kinetics and product detection,” *Review of Scientific Instruments* **82**, 124102 (2011).
- ³¹C. Abeysekera, B. Joalland, N. Ariyasingha, L. N. Zack, I. R. Sims, R. W. Field, and A. G. Suits, “Product branching in the low temperature reaction of CN with propyne by chirped-pulse microwave spectroscopy in a uniform supersonic flow,” *The journal of physical chemistry letters* **6**, 1599–1604 (2015).
- ³²B. Schläppi, J. H. Litman, J. J. Ferreiro, D. Stapfer, and R. Signorell, “A pulsed uniform laval expansion coupled with single photon ionization and mass spectrometric detection for the study of large molecular aggregates,” *Physical Chemistry Chemical Physics* **17**, 25761–25771 (2015).
- ³³D. B. Atkinson and M. A. Smith, “Design and characterization of pulsed uniform supersonic expansions for chemical applications,” *Review of scientific instruments* **66**, 4434–4446 (1995).
- ³⁴J. M. Oldham, C. Abeysekera, B. Joalland, L. N. Zack, K. Prozumant, I. R. Sims, G. B. Park, R. W. Field, and A. G. Suits, “A chirped-pulse fourier-transform microwave/pulsed uniform flow spectrometer. i. the low-temperature flow system,” *The Journal of chemical physics* **141**, 154202 (2014).
- ³⁵E. Jiménez, B. Ballesteros, A. Canosa, T. Townsend, F. Maigler, V. Napal, B. Rowe, and J. Albaladejo, “Development of a pulsed uniform supersonic gas expansion system based on an aerodynamic chopper for gas phase reaction kinetic studies at ultralow temperatures,” *Review of Scientific Instruments* **86**, 045108 (2015).
- ³⁶A. Canosa, A. Ocaña, M. Antinolo, B. Ballesteros, E. Jiménez, and J. Albaladejo, “Design and testing of temperature tunable de laval nozzles for applications in gas-phase reaction kinetics,” *Experiments in Fluids* **57**, 152 (2016).
- ³⁷L. Biennier, S. Carles, D. Cordier, J.-C. Guillemin, S. D. Le Picard, and A. Faure, “Low temperature reaction kinetics of $\text{CN}^- + \text{HC}_3\text{N}$ and implications for the growth of anions in Titan’s atmosphere,” *Icarus* **227**, 123–131 (2014).
- ³⁸J. Bourgalais, N. Jamal-Eddine, B. Joalland, M. Capron, M. Balaganesh, J.-C. Guillemin, S. D. Le Picard, A. Faure, S. Carles, and L. Biennier, “Elusive anion growth in Titan’s atmosphere: Low-temperature kinetics of the $\text{C}_3\text{N}^- + \text{HC}_3\text{N}$ reaction,” *Icarus* **271**, 194–201 (2016).
- ³⁹B. Joalland, N. Jamal-Eddine, J. Klos, F. Lique, Y. Trolez, J.-C. Guillemin, S. Carles, and L. Biennier, “Low-temperature reactivity of $\text{C}_{2n+1}\text{N}^-$ anions with polar molecules,” *Journal of Physical Chemistry Letters* **7**, 2957–2961 (2016).
- ⁴⁰J.-L. Le Garrec, B. Rowe, J. L. Queffelec, J. B. A. Mitchell, and D. C. Clary, “Temperature dependence of the rate constant for the $\text{Cl}^- + \text{CH}_3\text{Br}$ reaction down to 23 K,” *Journal of Chemical Physics* **107**, 1021–1024 (1997).
- ⁴¹D. Smith and N. Adams, “The selected ion flow tube (sift): Studies of ion–neutral reactions,” in *Advances in Atomic and Molecular Physics*, Vol. 24 (Elsevier, 1988) pp. 1–49.
- ⁴²T. Speck, T. I. Mostefaoui, D. Travers, and B. R. Rowe, “Pulsed injection of ions into the CRESU experiment,” *International Journal of Mass Spectrometry* **208**, 73–80 (2001).
- ⁴³D. Douglas and J. B. French, “Collisional focusing effects in radio frequency quadrupoles,” *Journal of the American Society for Mass Spectrometry* **3**, 398–408 (1992).
- ⁴⁴More details regarding the rf ion guide combining different field-order distributions can be found in patent US9123517(B2).
- ⁴⁵G. A. Bird, “Molecular gas dynamics,” NASA STI/Recon Technical Report A **76** (1976).
- ⁴⁶D. Papanastasiou, A. Lekkas, E. Raptakis, and M. Sudakov, “Simulation of ion mobility and diffusion of sodium ions based on revised ion–molecule collision models,” in *Proceedings of the 60th ASMS Conference on Mass Spectrometry and Allied Topics* (American Society for Mass Spectrometry, 2012).

- ⁴⁷M. Tsuji, H. Kouno, K. Matsumura, T. Funatsu, Y. Nishimura, H. Obase, H. Kugishima, and K. Yoshida, "Dissociative charge-transfer reactions of Ar^+ with simple aliphatic hydrocarbons at thermal energy," *The Journal of Chemical Physics* **98**, 2011–2022 (1993).
- ⁴⁸C. Praxmarer, A. Hansel, W. Lindinger, and Z. Herman, "A selected-ion-flow-drift-tube study of charge transfer processes between atomic, molecular, and dimer ion projectiles and polyatomic molecules ethane, propane, and *n*-butane," *The Journal of Chemical Physics* **109**, 4246–4251 (1998).
- ⁴⁹S. Matsuoka and Y. Ikezoe, "Ion–molecule reactions and thermal decomposition of ions in nitrogen–oxygen alkane (C2–C8) mixtures studied by time–resolved atmospheric pressure ionization mass spectrometry," *The Journal of Physical Chemistry* **92**, 1126–1133 (1988).
- ⁵⁰P. F. Wilson, C. G. Freeman, and M. J. McEwan, "Reactions of small hydrocarbons with H_3O^+ , O_2^+ and NO^+ ions," *International Journal of Mass Spectrometry* **229**, 143–149 (2003).
- ⁵¹R. J. Shul, B. L. Upschulte, R. Passarella, R. G. Keesee, and A. W. Castleman, "Thermal energy charge-transfer reactions of argon ions (Ar^+ and Ar_2^+)," *The Journal of Physical Chemistry* **91**, 2556–2562 (1987).
- ⁵²P. R. Kemper and M. T. Bowers, "An improved tandem mass spectrometer – ion cyclotron resonance spectrometer," *International journal of mass spectrometry and ion physics* **52**, 1–24 (1983).
- ⁵³H. Chatham, D. Hils, R. Robertson, and A. Gallagher, "Reactions of He^+ , Ne^+ , and Ar^+ with CH_4 , C_2H_6 , SiH_4 , and Si_2H_6 ," *The Journal of chemical physics* **79**, 1301–1311 (1983).
- ⁵⁴D. Smith and N. Adams, "Charge–transfer reaction $\text{Ar}^+ + \text{N}_2 \rightleftharpoons \text{N}_2^+ + \text{Ar}$ at thermal energies," *Physical Review A* **23**, 2327 (1981).
- ⁵⁵W. Lindinger, F. Howorka, P. Lukac, S. Kuhn, H. Villinger, E. Alge, and H. Ramler, "Charge–transfer reaction $\text{Ar}^+ + \text{N}_2 \rightleftharpoons \text{N}_2^+ + \text{Ar}$ at near thermal energies," *Physical Review A* **23**, 2319 (1981).
- ⁵⁶C. Rebrion, B. Rowe, and J. Marquette, "Reactions of Ar^+ with H_2 , N_2 , O_2 , and CO at 20, 30, and 70 K," *The Journal of Chemical Physics* **91**, 6142–6147 (1989).
- ⁵⁷V. G. Anicich, "Evaluated bimolecular ion–molecule gas phase kinetics of positive ions for use in modeling planetary atmospheres, cometary comae, and interstellar clouds," *Journal of Physical and Chemical Reference Data* **22**, 1469–1569 (1993).
- ⁵⁸M. Hamdan, K. Birkinshaw, and N. Twiddy, "Energy dependence of the reactions of Ar^+ ($^2P_{1/2}$) and Ar^+ ($^2P_{3/2}$) with N_2 ," *International Journal of Mass Spectrometry and Ion Processes* **57**, 225–231 (1984).
- ⁵⁹E. E. Ferguson, "Vibrational quenching of small molecular ions in neutral collisions," *The Journal of Physical Chemistry* **90**, 731–738 (1986).
- ⁶⁰H. Böhringer, M. Durup-Ferguson, D. Fahey, F. Fehsenfeld, and E. Ferguson, "Collisional relaxation of vibrationally excited O_2^+ ions," *The Journal of Chemical Physics* **79**, 4201–4213 (1983).
- ⁶¹A. A. Viggiano and R. A. Morris, "Rotational and vibrational energy effects on ion–molecule reactivity as studied by the VT-SIFDT technique," *The Journal of Physical Chemistry* **100**, 19227–19240 (1996).
- ⁶²R. Derai, P. R. Kemper, and M. T. Bowers, "Effect of reactant ion internal and translational energy on the rate constants of the charge exchange reactions: $\text{CO}_2^+ + \text{O}_2 \rightarrow \text{O}_2^+ + \text{CO}_2$ and $\text{O}_2^+ + \text{O}_2 \rightarrow \text{O}_2 + \text{O}_2^+$," *The Journal of Chemical Physics* **82**, 4517–4523 (1985).